

## Supplementary information for

Geranyl ester components of volatile chemical  
products readily induce black carbon  
restructuring

*Christian A. Escritt, Habeeb H. Al-Mashala, and Elijah G. Schnitzler\**

Department of Chemistry, Oklahoma State University, Stillwater, OK 74078, USA

E-mail: [elijah.schnitzler@okstate.edu](mailto:elijah.schnitzler@okstate.edu).

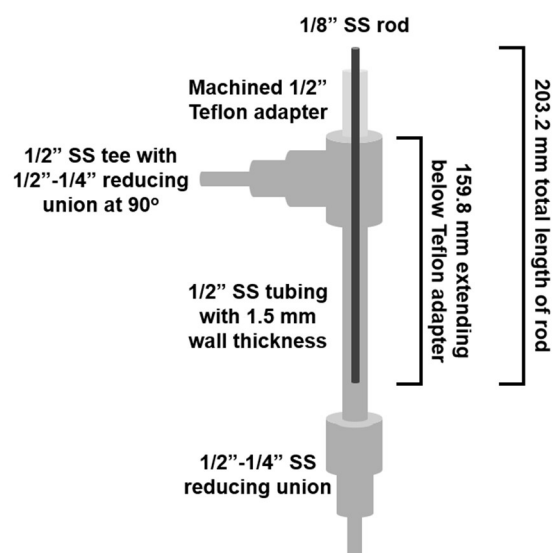


**Fig. S1.** Schematic of custom-built EPC. Particles enter at the bottom. The stainless-steel electrode lies at the radial center of the Teflon adapter but is shown in front of the other elements for clarity. Not shown, a machined stainless-steel cylinder, with set screws and the center drilled out, is used to connect the electrode to the lead of the high-voltage power supply; another machined Teflon fitting covers the electrical connection for safety.

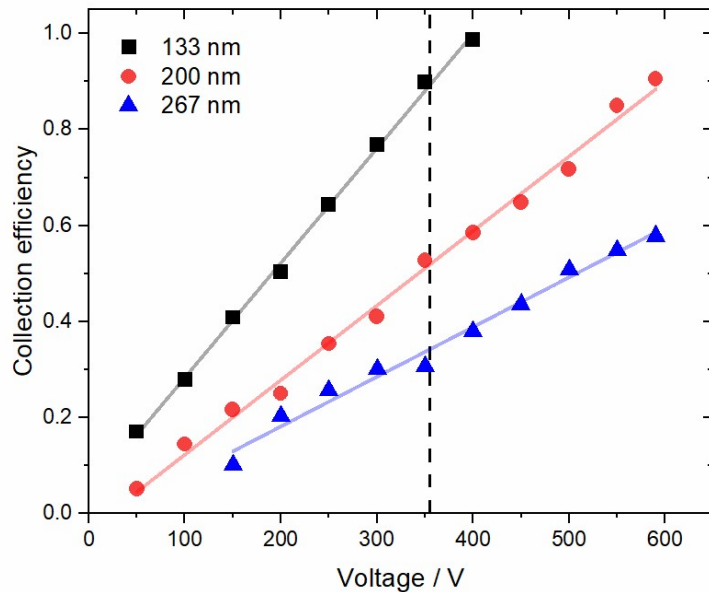


**Fig. S2.** Representative collection efficiencies as a function of negative voltage in the EPC for particles classified by DMA1 at three different mobility diameters. In all, nine different diameters were used in the calibration, as summarized in Fig. S3. The dashed line indicates the voltage used during the coating experiments, 355 V; the collection efficiency was determined at this voltage by counting particles with the CPC with the voltage on and off, alternately.

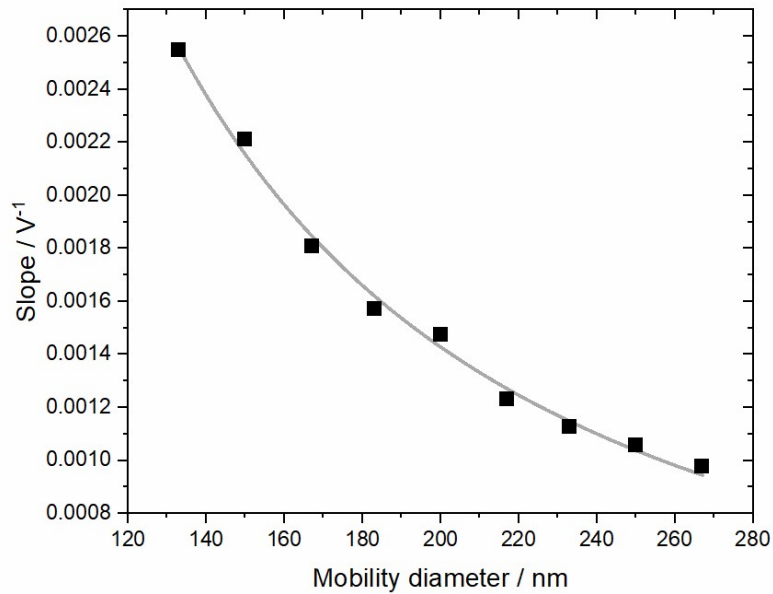


**Fig. S3.** Summary of the calibration of the EPC, in terms of the slopes, shown in Fig. S2, as a function of mobility diameter. The curve illustrates a power law fit to the calibration data.

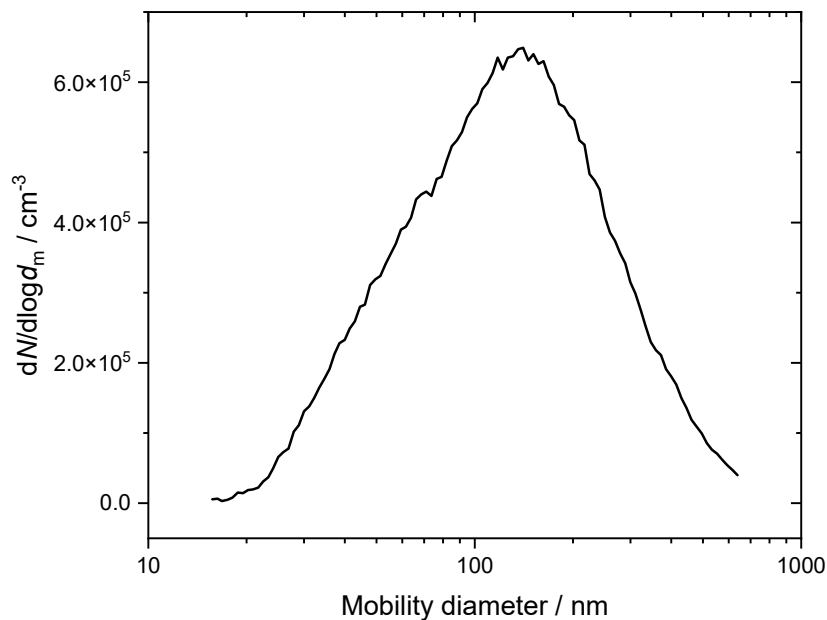


**Fig. S4.** Representative size distribution for the polydisperse particles from the miniature inverted soot generator, showing the burner is a suitable source of BC aggregates for use in the coating experiments. The burner produces BC with a geometric mean diameter of 120 nm; therefore, our choice of 200 nm, which is larger than the geometric mean diameter, minimizes the effect of multiply charged particles.

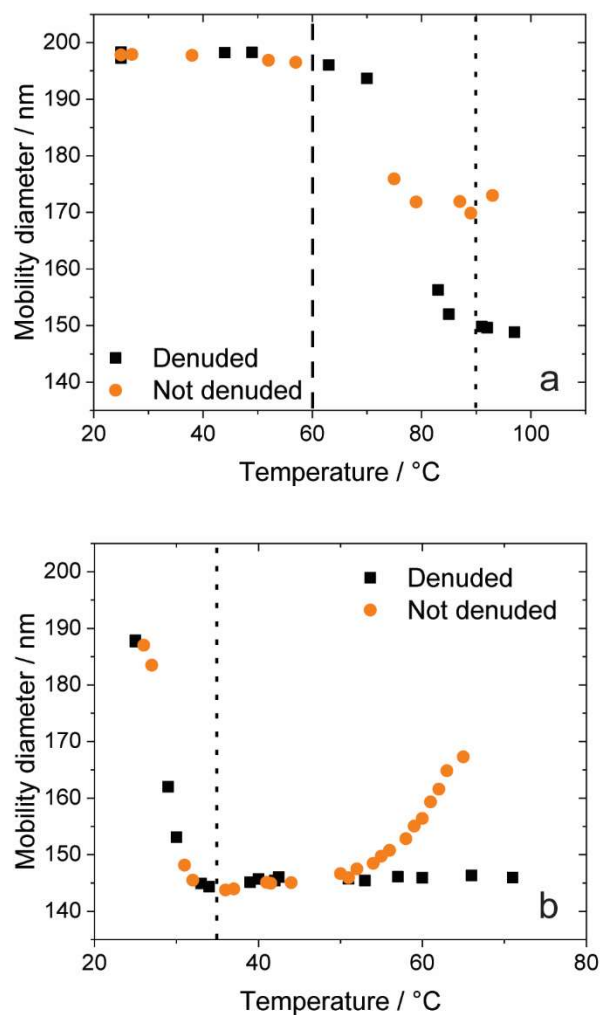


**Fig. S5.** Representative coating experiments using Setup 1 (i.e., the second DMA) with (a) dioctyl sebacate and (b) geranyl formate, showing evolution of the mobility diameter of particles with and without thermal denuding as a function of saturator temperature. The dashed line (a) denotes the onset of restructuring, i.e., the second stage of the experiment. The dotted line (a-b) denotes near-complete restructuring of the coated BC aggregates. Note the different scales on the x-axes of the two panels.

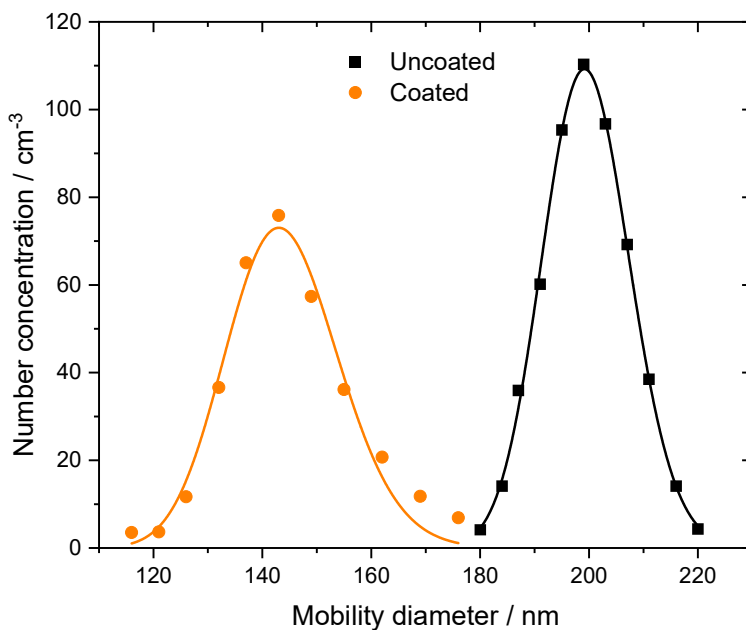


**Fig. S6.** Representative size spectra measured using Setup 1 (i.e., the second DMA) for monodisperse nascent BC before coating (i.e., centered at about 200 nm) and BC after coating with geranyl formate (i.e., centered at about 144 nm). This shift equates to a decrease of about 56 nm in mobility diameter or about 28% of the initial mobility diameter of the BC aggregates. This 28% decrease gives a diameter growth factor of about 0.72 at the fully restructured state, which was roughly consistent for all the geranyl compounds.

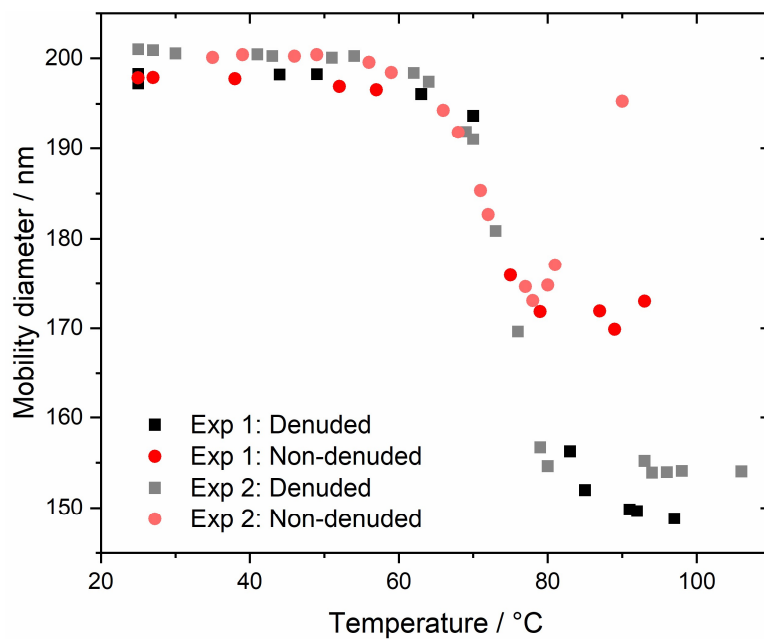


**Fig. S7.** Duplicate coating experiments using Setup 1 (i.e., the second DMA) for diocetyl sebacate.

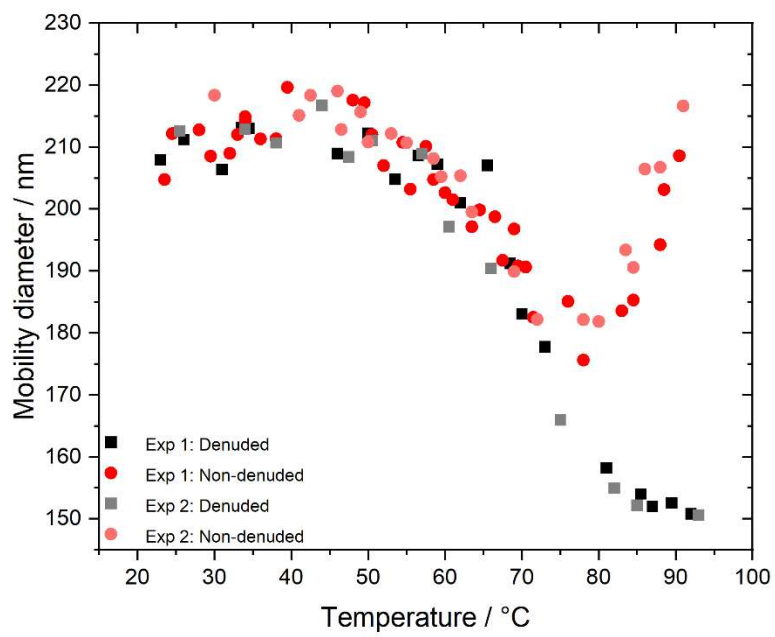


**Fig. S8.** Duplicate coating experiments using Setup 2 (i.e., the EPC) for diethyl sebacate.

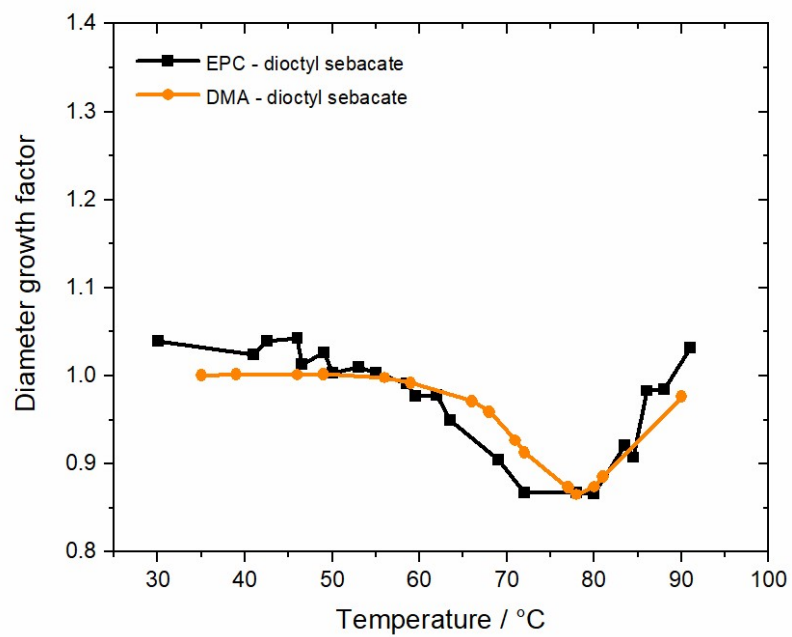


**Fig. S9.** Comparison of diameter growth factors for non-denuded aggregates coated with dioctyl sebacate measured using Setup 1 (i.e., the second DMA) versus Setup 2 (i.e., the EPC).

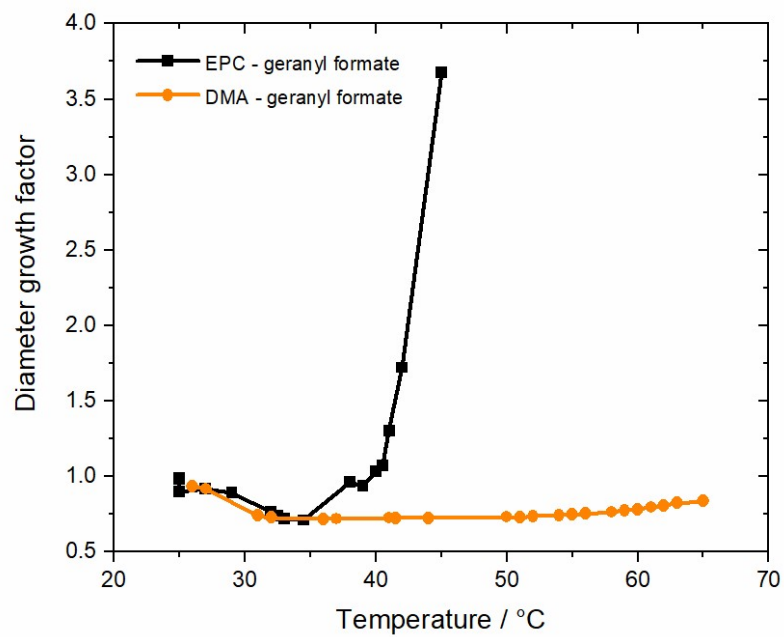


**Fig. S10.** Comparison of diameter growth factors for non-denuded aggregates coated with geranyl formate measured using Setup 1 (i.e., the second DMA) versus Setup 2 (i.e., the EPC).

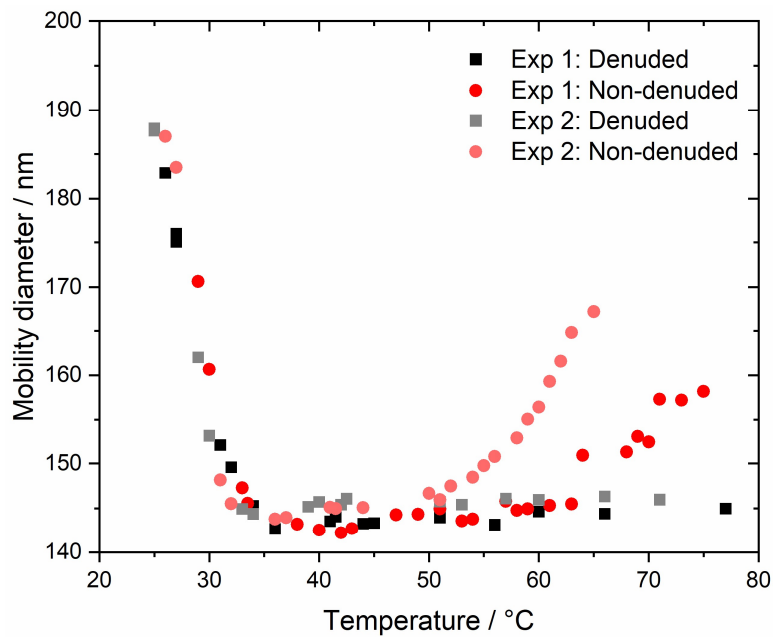


**Fig. S11.** Duplicate coating experiments using Setup 1 (i.e., the second DMA) for geranyl formate. Note that there are differences between the duplicate experiments in terms of the non-denuded mobility diameters at elevated saturator temperatures, as the conditions governing the coating volume can vary between experiments.

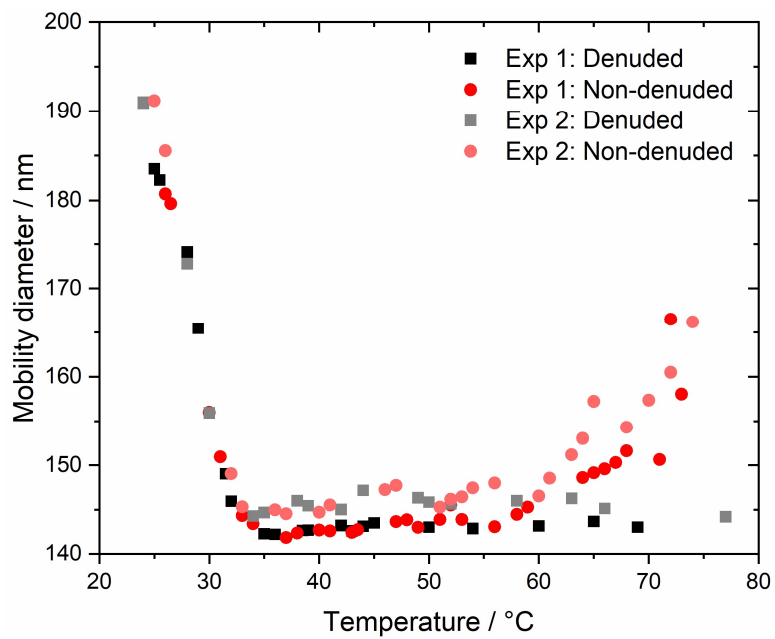


**Fig. S12.** Duplicate coating experiments using Setup 1 (i.e., the second DMA) for geranyl acetate.

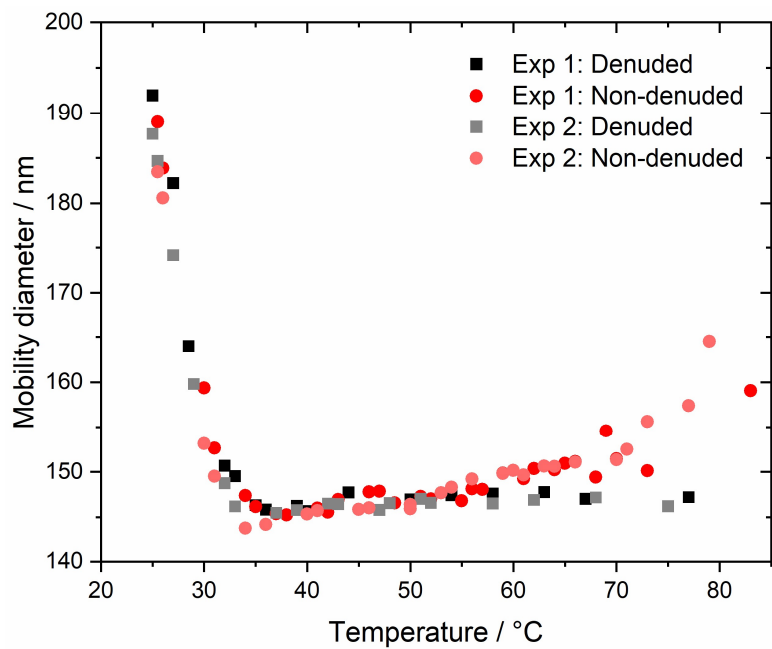


**Fig. S13.** Duplicate coating experiments using Setup 1 (i.e., the second DMA) for geranyl propionate.

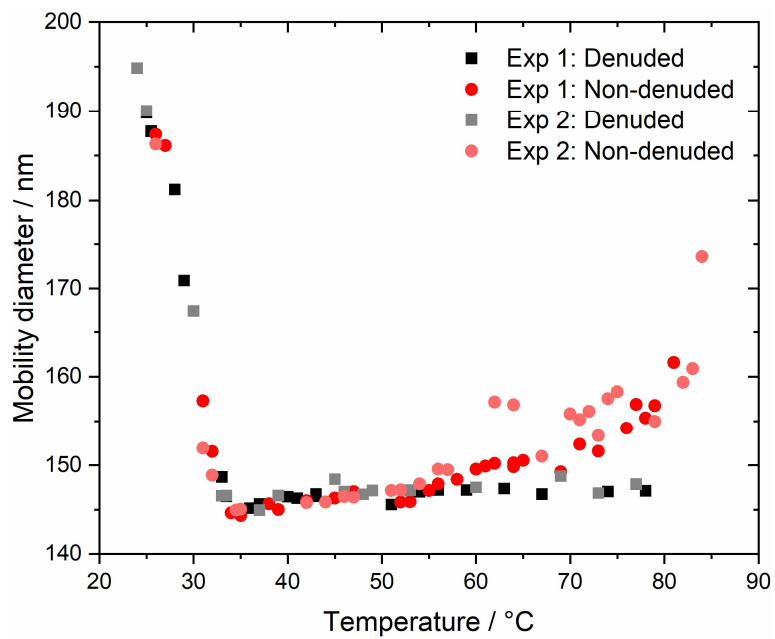


**Fig. S14.** Duplicate coating experiments using Setup 1 (i.e., the second DMA) for geranyl butyrate.

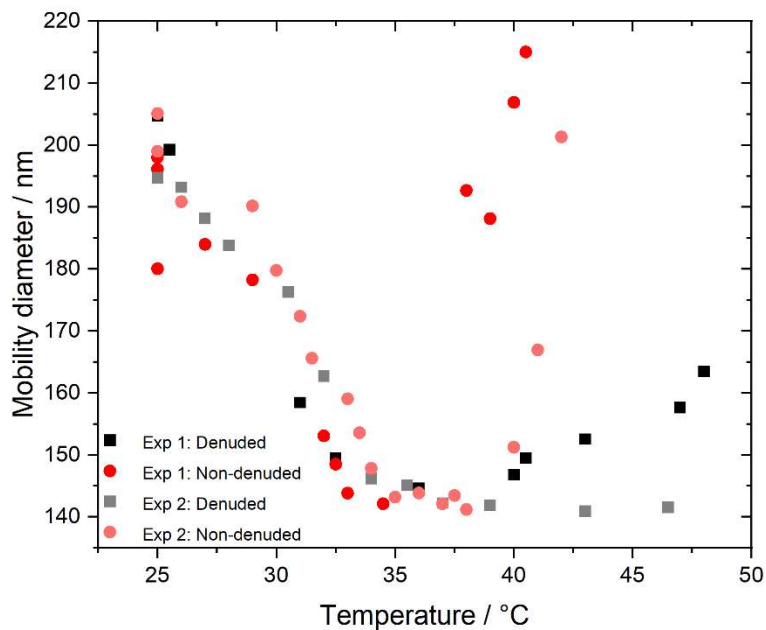


**Fig. S15.** Duplicate coating experiments using Setup 2 (i.e., the EPC) for geranyl formate. Again, note that there are differences between the duplicate experiments in terms of the non-denuded mobility diameters at elevated saturator temperatures, as the conditions governing the coating volume can vary between experiments. These differences are accounted for in Fig. 5 in the main text by using volume growth factor,  $G_{fv}$ , as the independent variable.

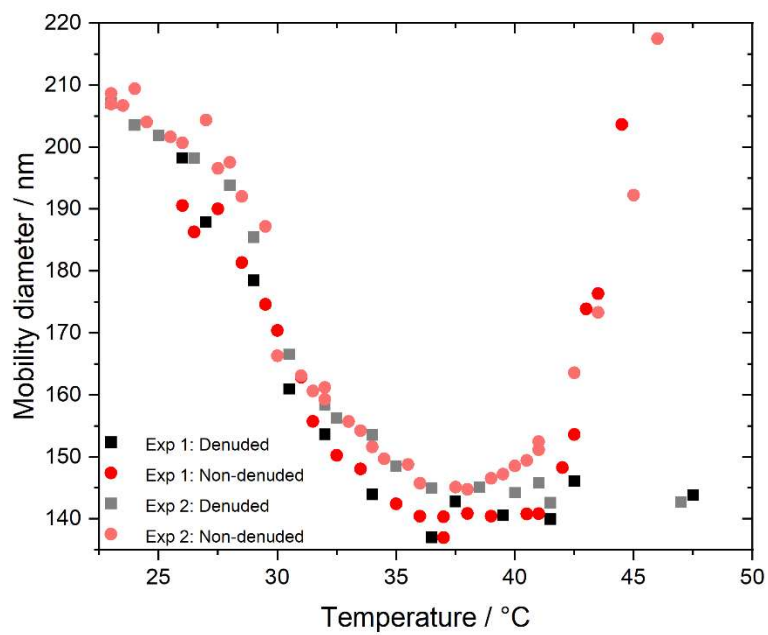


**Fig. S16.** Duplicate coating experiments using Setup 2 (i.e., the EPC) for geranyl acetate.

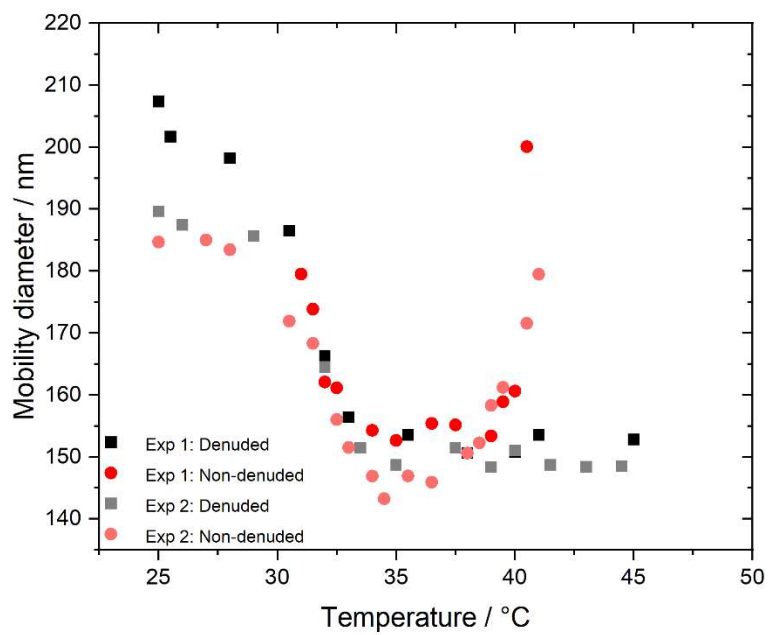


**Fig. S17.** Duplicate coating experiments using Setup 2 (i.e., the EPC) for geranyl propionate.

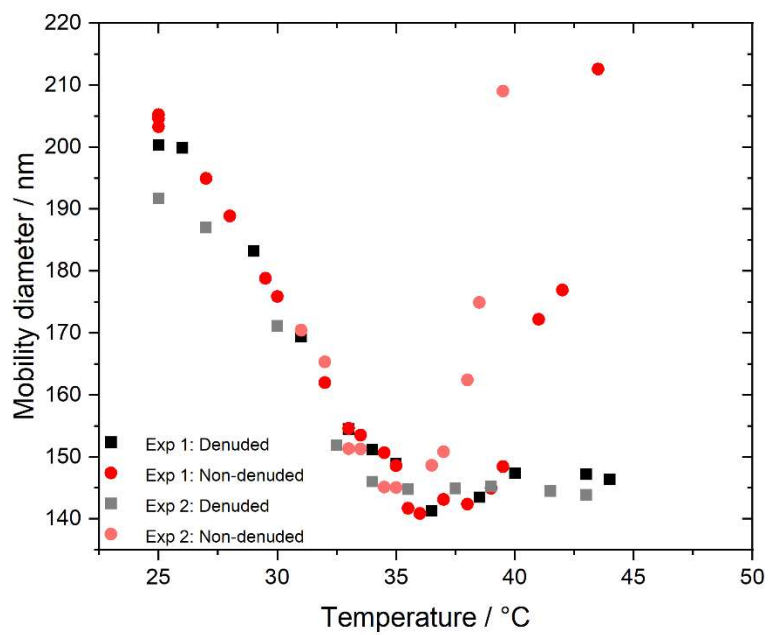


**Fig. S18.** Duplicate coating experiments using Setup 2 (i.e., the EPC) for geranyl butyrate.

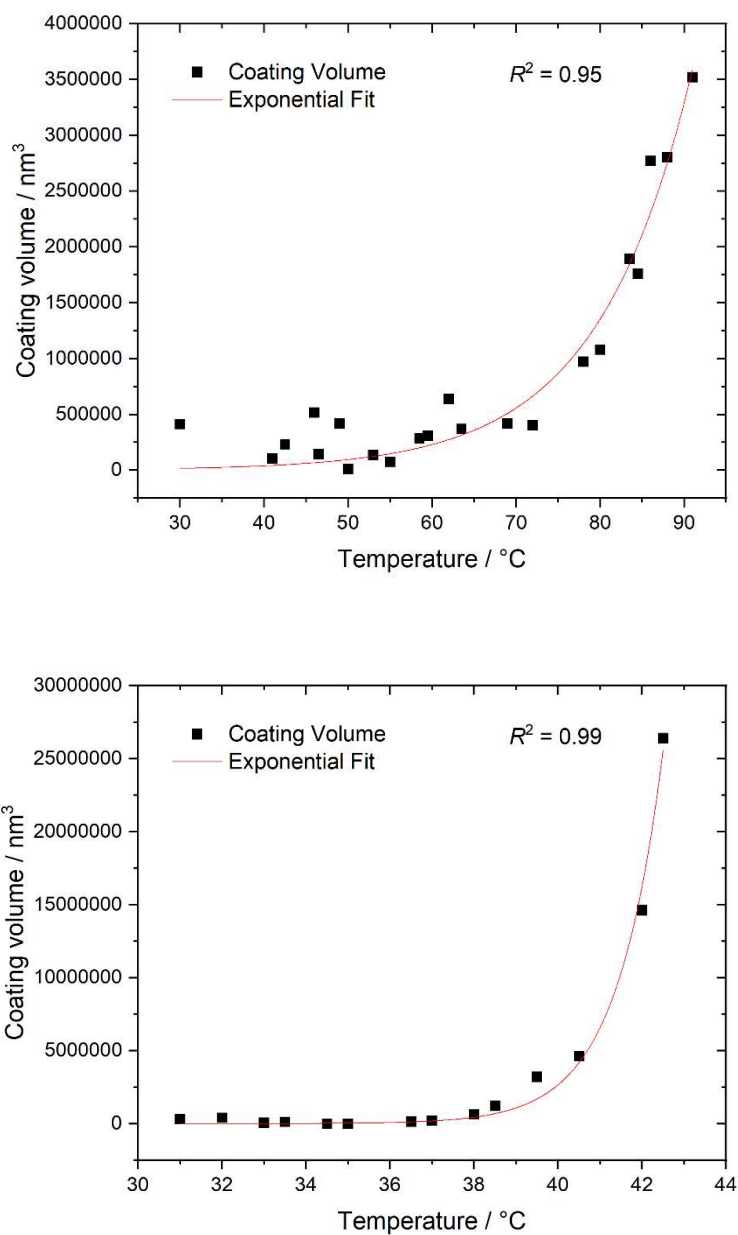


**Fig. S19.** Representative exponential fits to coating volume during the third stage of representative experiments with (top) diocetyl sebacate and (bottom) geranyl butyrate as a function of saturator temperature, obtained by taking the volume of coated particles minus the volume of the denuded BC cores, which were calculated using the particles mobility diameters when the BC was completely restructured.

**Table S1.** Surface tension for all coating materials used in BC experiments.

<b>Compound</b>	<b>GB</b>	<b>GP</b>	<b>GA</b>	<b>GF</b>	<b>DS</b>
Surface tension (mN m <sup>-1</sup> )	29.1	28.8	28.5	28.9	33.3

**Table S2.** Single parameter values,  $\chi$ , coating volume fractions, and capillary and uniform condensate volumes predicted for different reduced supersaturations,  $\zeta$ , of geranyl butyrate at room temperature (298.15 K), using the online Capillary Condensation Model, based on its surface tension (29.1 mN m<sup>-1</sup>), density, molar mass, and saturated vapor pressure (0.465 Pa) and a residence time of 1 s.

$\zeta$	$\chi$	Coating volume fraction	Capillary condensate $V$ per point contact (m <sup>3</sup> )	Uniform condensate $V$ per primary particle (m <sup>3</sup> )
1	0.47	0.998	$4.23 \times 10^{-24}$ <sup>a</sup>	$3.69 \times 10^{-21}$ <sup>b</sup>
0.1	4.7	0.234	$2.51 \times 10^{-24}$ <sup>a</sup>	0 <sup>c</sup>
0.01	47	0.102	$9.28 \times 10^{-25}$ <sup>a</sup>	0 <sup>c</sup>
0.001	470	0.0955	$8.64 \times 10^{-25}$ <sup>a</sup>	0 <sup>c</sup>

<sup>a</sup> These values do not change in time after 0.1 s in the simulations.

<sup>b</sup> This value changes with time of simulation; since  $\chi$  is small and uniform condensation is favored, at a constant supersaturation, the coating volume grows linearly in time. Any time after the capillary condensate volume is steady, i.e., 0.1 s, serves to illustrate the distribution of coating volume.

<sup>c</sup> These values are constant throughout the simulations.